Kalman Filter Based Adaptive Reduction of Motion Artifact from Photoplethysmographic Signal

S. Seyedtabaii, and L. Seyedtabaii

***Abstract*—**Artifact free photoplethysmographic (PPG) signals are necessary for non-invasive estimation of oxygen saturation (SpO2) in arterial blood. Movement of a patient corrupts the PPGs with motion artifacts, resulting in large errors in the computation of Sp02. This paper presents a study on using Kalman Filter in an innovative way by modeling both the Artillery Blood Pressure (ABP) and the unwanted signal, additive motion artifact, to reduce motion artifacts from corrupted PPG signals. Simulation results show acceptable performance regarding LMS and variable step LMS, thus establishing the efficacy of the proposed method.

***Keywords*—**Kalman filter, Motion artifact, PPG, Photoplethysmography.

I. Introduction

PHOTOPLETHYSMOGRAPH (PPG) signal is very useful non-invasive monitoring technique to measure indirectly heart rate, blood oxygen saturation (SpO2) with a little constraint. Nevertheless, its measuring technique needs to have a low failure rate and must report minimal false alarms.

However, PPG signal is contaminated by motion artifact and ambient light variation during recordings**.** Changes in ambient light can be rejected using the emission of modulation signals from an infrared emitter [1]. The most troublesome problem with dynamic PPG measurements is motion artifact, mainly resulting from air gap between sensor and skin, which it can lead to a poor estimation of physiological parameters from the recordings. Even slight movement of the patient would then invariably disturb the contact between the sensor and the patient's body, corrupting the PPGs obtained during such periods with motion artifacts, resulting in erroneous estimation of SPO2. Motion artifact is mainly low frequency interference, and it is random in nature. Thus, elimination of this motion artifact through fixed filtering techniques is not advisable due to both the in-band nature of interference and overlapping of the most important frequency spectrum of the PPG signal, between 0.2-35 Hz [2].

In most recent developments in PPG motion artifact reduction, [3] reports a method based on exploiting the quasi-periodicity of the PPG signal and the independence between the PPG and the motion artifact signals. In [4] motion artifact reduction in PPG is achieved with a novel nonlinear methodology. [5] suggests the scaled Fourier Linear Combiner (SFLC) to remove effectively the motion artifacts as well as background noise by exploiting the quasi-periodicity of the PPG signal and the independence between the PPG and the motion artifact signals.

Apart from these methods, from years, continuous processing techniques using adaptive filters, to suppress the effect of motion artifact [1-6-7], has been under investigation, because, these techniques allow fast response times, does not need signal segmentation, and is able to continue processing under moderate artifact conditions. In [1] the experimental results of implementing LMS and variable step (VS) LMS are introduced and illustrates the vsLMS, to some extent, acceptable performance.

In this paper, a noticeable improvement to [1] is reported by introducing an innovative modeling into Kalman Filter, identifying both the ABP signal and the motion artifact models, leading to an algorithm that outperforms the already used adaptive techniques.

In section 2 the nature of PPG signal and motion artifact effects are analyzed. A new formulation for motion artifact reduction, to fit Kalman filter structure, comes in section 3. Kalman filter equations are presented in section 4. Simulation results are illustrated in section 5 and lastly section 6 contains conclusion.

II. PPG Signal and Motion Artifact

Cardiac output (CO) can be visualized by arterial blood pressure (ABP) waveform. According to the windkessel model, cardiac output (CO) may be modeled by a single pole system as its impulse response (ABP) indicates in Fig. 1. ABP should decay like a pure exponential during each diastolic interval with a time constant equal to the product of the total peripheral resistance (TPR) and the nearly constant arterial compliance (AC) [8].

Manuscript received December 29, 2007. This work was supported in part by the Engineering and Technology Research Center (ETRC) of Shahed University.

Saeed Seyedtabaii is with the Shahed University, Tehran, Iran (corresponding author: e-mail: stabaii@shahed.ac.ir).

Layla Seyedtabaii is with the Qum University of Medical Science, Qum, Iran (e-mail: leiladrml@yahoo.com).

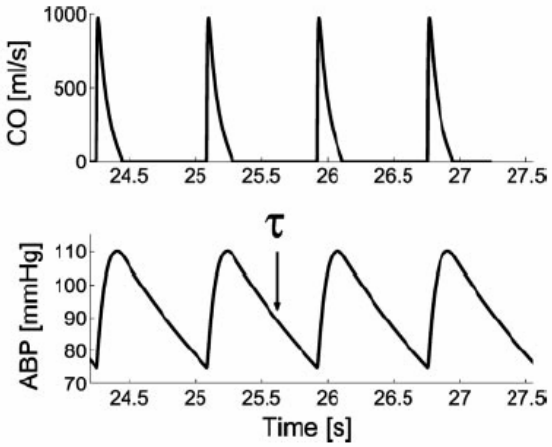

Fig. 1 Cardiac output (CO) and arterial blood pressure (ABP) waveforms [8]

This pulse contour analysis proved to be successful when applied to ABP waveforms measured centrally in the aorta, because the diastolic interval of these waveforms can resemble an exponential decay after incisura. Indeed, it is well known that the contour of the arterial pulse changes significantly as it traverses through the arterial tree. The reason is that the arterial tree is not simply a lumped system as the windkessel model suggests, but rather a complicated distributed system with impedance mismatches throughout due to vessel tapering, bifurcations, and caliber changes. Thus, the diastolic (and systolic) intervals of peripheral ABP waveforms are corrupted by complex wave reflections that occur at each and every site of impedance mismatch. The above pulse contour analysis therefore cannot be applied to measured peripheral ABP waveforms [9] like the one measured at finger tip by PPG.

PPG probe consisted of two pairs of LED and a phototransistor working at two different wavelengths. In one of them, Infrared light of 935 nm from a GaAs LED is used as an emitter, and a NPN silicon phototransistor was used as a detector for receiving the reflected light from the tissues. The intensity of LED light transmitted across the fingertip, for example, varies as shown in Fig. 2. A pulsatile signal, which varies in time with the heartbeat, is superimposed on a d.c. level. The amplitude of this cardiac pulsatile signal is approximately 1% of the d.c. level. The d.c. part that is due to the attenuation of light by the body segment can be split into the three independent components shown in Fig. 2: arterial blood, venous blood and tissues.

The majority of light produced by a PPG probe is scattered by tissue, venous blood and arterial blood. A small proportion of light experiences variable scatter due to the pulsation of arterial blood. Some proportion of this light is detected and contains the signature of the pulsatile component of arterial blood flow. From Fig. 2, it is apparent that the proportion of the detected light that contains the pulsatile component is a fraction of the total received light [10].

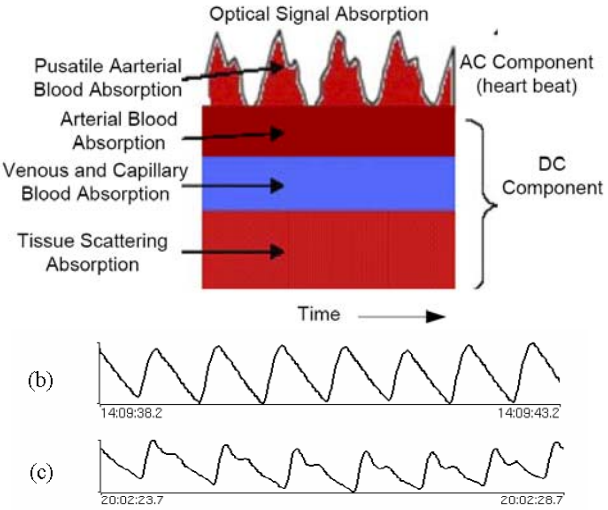

Fig. 2 Various attenuations in Transmission of light through finger and its typical pulsatile detected signal [10]

The pulsatile waveform may be viewed as an output of a system excited by heart beat impulse. The pulsatile waveform, depicted in Fig. 2, indicates that a single pole system can not adequately model it, instead at least a system of 2 real poles and a pair of complex poles is needed to form a suitable model.

In dynamic PPG measurements, motion artifact due to motion of finger, causes variation in DC component adding unwanted variations to the fore mentioned pulsatile signal resulting from heart blood pumping. This variation corrupts the signal making reduction, mainly resulting from the air gap between the sensor and the skin, and it can lead to a poor estimation of physiological parameters from the recordings. Motion artifact is mainly low frequency interference, additive type and it is random in nature [1]. According to the experiments conducted in [1], d(n) is highly correlated with x(n) and s(n) is less correlated with both d(n) and x(n). Then, the basic assumption of the adaptive filter is, therefore satisfied.

III. Case Formulation

The primary sensor, PPG probe, detects y(n)=s(n)+d(n), where s(n) is the PPG signal and d(n) is the additive motion artifact. The desired idea is removal of d(n) from y(n) and extracting the estimation of s(n), namely, $\hat{s}(n)$.This is depicted in Fig. 3.

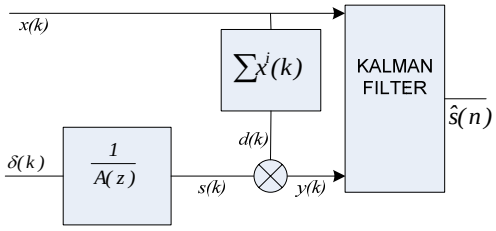

Fig. 3 Kalman Filter Based Motion Artifact Removal Scheme

The reference sensor detects noise component, x(n), which provides a correlated version of the motion artifact, d(n). Accelerometers, strain gauges, and Ag-AgCl paste electrodes are used to detect motion artifact, but optoelectronic sensors for the reasons of simplicity, economic and size may be viewed preferable [1].

Based on the discussion presented in section 2, It is assumed that s(n) to be impulse response of an all pole filter. A filter, that its output mimics the ABP signal at fingertip. As mentioned earlier, this filter, to model the case appropriately, needs to be of order 4, but an order 2 filter may also be able to handle the job of artifact reduction. Thus, the chosen model is

$$\frac{1}{A(z)} = \frac{k}{1 + a_1 z^{-1} + a_2 z^{-2}}$$

Selection of this model means that s(n) is assumed to be the result of summation of its past values

$$s(k) = \sum_{i=1}^{2} a_i s(k-i) + p(k)$$

where p(k) is the periodic heart beat. The static behavior of the motion artifact, on the other hand, can be represented, by a polynomial equation

$$d(k) = \sum_{i=1}^{N} b_i x^i(k)$$

where the degree N in the expansion, reflects nonlinearity complexity. Therefore, the overall signal and motion artifact is

$$y(k) = \sum_{i=1}^{2} a_i s(k-i) + p(k) + \sum_{i=1}^{N} b_i x^i(k)$$

With the assumption of stationarity for the overall system, the general form of the update equations for the estimation of the parameters is

$$X_{k+1} = AX_k = \begin{bmatrix} a_{1k+1} \\ a_{2k+1} \\ b_{Nk+1} \\ . \\ b_{2k+1} \\ b_{1k+1} \end{bmatrix} = [I] \begin{bmatrix} a_{1k} \\ a_{1k} \\ b_{Nk} \\ . \\ b_{2k} \\ b_{1k} \end{bmatrix} \quad (1)$$

$$y_k = C_k X_k = \begin{bmatrix} s_{k-1} & s_{k-2} & x_k^N & . & . & x_k \end{bmatrix} X_k + W_k \quad (2)$$

where X_k is an n-dimensional vector of unknown parameters, I the n-dimensional identity matrix, Y_k is the scalar valued measurement, C_k is the vector of measurement history and W_k is assumed as measurement noise. Since s(k) is not measurable, the appropriate choice, its last estimation $\hat{s}(k)$ is used in its place. Thus, a change in the formulation is required to make it implementable. Therefore, the estimation of the true ABP waveform is calculated from

$$\hat{s}(k) = y(k) - \hat{d}(k) = y(k) - \sum_{i=1}^{N} \hat{b}_i x^i(k)$$

leading to a new definition for vector C_k

$$y_k = C_k X_k = \begin{bmatrix} \hat{s}_{k-1} & \hat{s}_{k-2} & x_k^N & . & . & x_k \end{bmatrix} X_k + W_k$$

Now, the case is in a form that Kalman filter can be used to estimate $\hat{X}$, minimizing the variance of the error ($y - C\hat{X}$) that eventually yields estimation of s, namely $\hat{s}$.

IV. Kalman Filter Solution

The solution for the State Space model presented in (1) and (2) is determined using an iterative approach as follows [11]:

$$K_k = AP_k C_k^T / (C_k P_k C_k' + \varepsilon)$$
$$\hat{X}_{k+1} = A\hat{X}_k + K_k (y_k - C_k \hat{X}_k)$$
$$P_k = (A - K_k C_k) P_k (A - K_k C_k)^T + \varepsilon K_k K_k^T$$

where K is the Kalman gain, k is the discrete time sample, P is the uncertainty covariance matrix and $0<\varepsilon \leq 1$ is added to model measurement noise.

V. Simulations

To study the efficacy of the proposed method and evaluate its performance, simulations based on previously known parameters and systems are conducted. The PPG signal is generated by a system of 4 poles

$$\frac{k}{A(z)} = \frac{k}{(s+3)(s+6)(s^2+14s+1000)}$$

The motion artifact impact on the ABP signal is assumed to be an unknown nonlinear static function and it is approximated by a polynomial of order 2.

For reconstruction of s(n) from contaminated y(n), Kalman filter arrangement is pursued to minimize the variance of the error between the measured output y_k and the estimated output $\hat{y}_k$

$$e(k) = y(k) - \hat{y}(k) = y(k) - C_k X_k$$

Fig. 3(a) shows the original signal produced for simulation purpose. Fig. 3(b) is the PPG signal affected by a static square motion artifact. Fig. 3(c) is the estimated signal using the proposed method. Fig. 3(d) is the error signal reflecting both the estimation error and the heart beat impulse. The convergence time for the KF approach depends on the initial value of P. The presented graph is for P=10*I were I is the

identity matrix. With this value of P algorithm performs enough fast to be able to confront normally induced motion artifacts. In the case of PPG artifact removal, speed of convergence is a compulsory must, since the algorithm should be able to cope with ordinary motion artifact speed resulting from, enough fast, finger movement.

In these simulations, without loss of generality, the original and the motion artifact signal spans are assumed to be limited to 1 and the mean value of both y and x signal are removed. The estimated A(z) is

$$\hat{A}(z) = 1 - 1.9759z^{-1} + 0.9827z^{-2}$$

The best result that we could acquire implementing vsLMS is shown in Fig. 3 (e), resulting from setting μ=0.5, under the fore mentioned ranges of input signals. Comparing graph "c" and graph "e" with regard to the original signal graph "a", clearly shows how well the proposed KF method performs. Since the graphs illustrate clearly the performance, no need for a quantitative measure, based on any type of distance measurement, was felt.

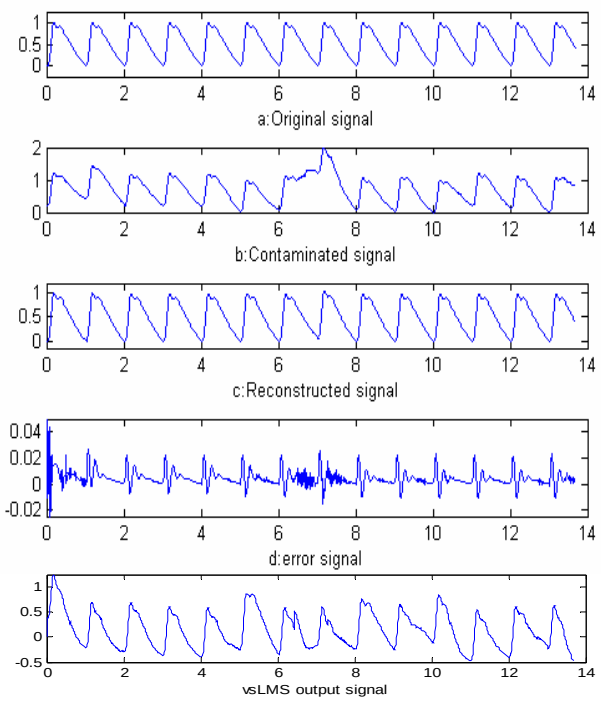

Fig. 4 a) Original simulated PPG signal, b) PPG signal contaminated with motion artifact, c) KF estimated signal, d) estimation error and e) estimation using vsLMS

VI. Conclusion

With the implementation of a special data structure into Klaman filter, the estimation of the true PPG signal is obtained. Finger movement is simulated and used as a reference noise. PPG contaminated signal, containing both the ABP related signal and the disturbance effects, is used as a primary signal. While the PPG signal is severely deformed by motion artifact, the proposed algorithm is still able to extracts the main signal from a type of disturbance that is in band with the main signal and it cannot be filtered with conventional type of filters. The performance of the proposed method is excellent but also, for a matter of comparison, is compared with what a well-tuned variable step LMS adaptive filter may yield.

References

[1] K. W. Chan and Y. T. Zhang, "Adaptive Reduction of Motion Artifact from Photoplethysmographic Recordings using a Variable Step Size LMS Filter," Sensors, 2002. Proceedings of IEEE, Volume: 2, pp. 1343-1346.

[2] P. D. Larsen, M. H. Mohana Thirchelvarn, and Duncan C. Galletly, "Spectral analysis of AC and DC components of the pulse photoplethysmogrphy at rest and during induction of anesthesia," International Journal of Clinical Monitoring and Computing, 1997, 14, pp.89-95.

[3] B. S. Kim and S. K. Yoo, "Motion artifact reduction in photoplethysmography using independent component analysis," IEEE Transactions on Biomedical Engineering, Volume 53, Issue 3, March 2006 Page(s): 566 – 568.

[4] M. J. Hayes and P. R. Smith, "Artifact Reduction in Photoplethysmography, "Applied Optics, Vol. 37, Issue 31, pp. 7437-7446

[5] Y Yan, C Poon and f Y Zhang, "Reduction of motion artifact in pulse oximetry by smoothed pseudo Wigner-Ville distribution," Journal of NeuroEngineering and Rehabilitation 2005, 2:3

[6] J. B. Evans and B. Liu, "Variable step size methods for the LMS adaptive algorithms," IEEE Int. Symp. Circuits. Syst. Proc, 1987, pp.422-425.

[7] E. W. Harris and C.D.M.a.B.F.A., "A variable step (VS) adaptive filter algorithm," IEEE Transactions on Biomedical Engineering, 1986, Vol. 34, pp.309-316.

[8] R. Mukkamala, AT Reisner, HM Hojman, RG Mark, and RJ Cohen, "Continuous cardiac output monitoring by peripheral blood pressure waveform analysis," IEEE Trans Biomed Eng, 53: 459–467, 2006.

[9] Z Lu and R Mukkamala, "Continuous cardiac output monitoring in humans by invasive and noninvasive peripheral blood pressure waveform analysis," J Appl Physiol 101: 598–608, 2006;

[10] N Townsend, M. Term, "Pulse Oximetry," Medical Electronics, 2001, pp.35-45

[11] Bernard Widrow, J.M.M., Michael G. Larimore and C.Richard Johnson, "Adaptive noise canceling: Principles and applications," Proceedings of IEEE, Dec. 1975, Vo163, pp.1692-1716.

[12] S. Haykin, Adaptive Filter Theory. Fourth Edition. Prentice-Hall, Inc., Englewood Cliffs, NJ, 2002.